Image charge screening: A new approach to enhance magnetic ordering temperatures in ultrathin correlated oxide films

S. Altieri,[1] M. Finazzi,[2] H. H. Hsieh,[3] M. W. Haverkort,[4] H.-J. Lin,[5] C. T. Chen,[5] S. Frabboni,[1,6] G. C. Gazzadi,[1] A. Rota,[6] S. Valeri,[1,6] and L. H. Tjeng[4]

[1]*CNR-INFM National Center on NanoStructures and BioSystems at Surfaces (S3), via G. Campi 213/a, 41100 Modena, Italy*

[2]*Dipartimento di Fisica, Politecnico di Milano, Piazza Leonardo da Vinci 32, 20133 Milano, Italy*

[3]*Chung Cheng Institute of Technology, National Defense University, Taoyuan 335, Taiwan*

[4]*II. Physikalisches Institut, Universität zu Köln, Zülpicher Str. 77, D-50937 Köln, Germany*

[5]*National Synchrotron Radiation Research Center, Hsinchu 30077, Taiwan*

[6]*Department of Physics, University of Modena and Reggio Emilia, via G. Campi 213/A, I-41100 Modena, Italy*

(Received 19 March 2009; published 26 May 2009)

We have tested the concept of image charge screening as a new approach to restore magnetic ordering temperatures and superexchange interactions in correlated oxide ultrathin films. Using a three-monolayer NiO(100) film grown on Ag(100) and an identically thin film on MgO(100) as model systems, we observed that the Néel temperature of the NiO film on the highly polarizable metal substrate is 390 K while that of the film on the poorly polarizable insulator substrate is below 40 K. This demonstrates that screening by highly polarizable media may point to a practical way toward designing strongly correlated oxide nanostructures with greatly improved magnetic properties.

DOI: 10.1103/PhysRevB.79.174431 PACS number(s): 75.70.−i, 75.30.Et, 78.70.Dm

I. INTRODUCTION

Transition-metal oxides exhibit many spectacular magnetic and electrical properties including high-temperature superconductivity and colossal magnetoresistance[1] making them particularly promising for nanoscience technology applications. An acute issue in the field of nanoscience, however, is the strong reduction of the relevant critical or ordering temperatures due to well-known finite-size effects.[2–8] If ways could be found to compensate for these reductions, one would immediately enlarge the materials basis for nanotechnology. Current approaches to overcome these problems include the use of chemical doping, pressure, and strain.[9–14]

The concept of finite-size scaling is well established in the realm of ultrathin metallic ferromagnetic films, where strong changes in the magnetic ordering temperature T_c have been reported in the literature.[2,15–18] In these systems, reduced dimensionality effects might be partially compensated by modifying the film environment, as demonstrated by decorating ferromagnetic thin films with various adsorbates.[19,20]

In the present paper we explore the possibility to induce substantial modifications of the Néel temperature in ultrathin films of antiferromagnetic (AF) oxide insulators, for which the magnetism is well understood in terms of superexchange interactions.[21–24] We propose to exploit image charge screening as a method to compensate finite-size phenomena and to restore magnetic ordering temperatures in a highly correlated oxide compound well beyond the capability of conventional methods.[9–14] The basic idea is to bring the material in the close proximity of a strongly polarizable medium. The relevant exchange and superexchange interactions, and thus the related magnetic ordering temperatures, can then be substantially amplified by reducing the energies of the underlying virtual charge excitations as a result of the image charge–like screening by the polarizable medium.[25–29]

To prove this concept we have chosen to measure the Néel temperature T_N of a three-monolayer (ML) NiO film epitaxially grown on a MgO(100) substrate and of an equally thin film on Ag(100). NiO films on MgO and on Ag are ideal model systems for this study because of their simple crystal structure and well-characterized growth properties.[30–37] They have a rocksalt crystal structure with lattice constant a_{MgO}=4.212 Å and a_{NiO}=4.176 Å, respectively, corresponding to a lattice misfit of about 1%. This ensures a perfect layer-by-layer epitaxial growth of NiO(100) on MgO(100), with a NiO(100) film surface roughness of about 0.1 Å.[30,31] Silver has a cubic *fcc* structure with a lattice constant a_{Ag}=4.086 Å and a mismatch with respect to NiO of about 2%. When misfit dislocations are avoided by keeping the film thickness below the critical thickness for strain relaxation (about 30 ML for NiO/Ag[32]) as done in the present work, then NiO(100) films grow on Ag(100) in a nicely layered and coherent mode with a sharp interface. This was already demonstrated by Kado,[33,34] but it has also been verified on our samples as we will show below.

II. SAMPLE PREPARATION AND CHARACTERIZATION

The NiO/MgO and NiO/Ag samples were prepared and comparatively studied *in situ* under identical conditions using the Cologne University molecular-beam epitaxy–x-ray absorption spectroscopy (MBE-XAS) setup at the Dragon beam line of the National Synchrotron Radiation Research Center in Taiwan. Microscopy experiments were performed at the Modena University. Stoichiometric NiO films were grown by atomic-oxygen-assisted reactive deposition[37] on a highly ordered Ag(100) and on cleaved MgO(100) single crystals kept at 463 K in a background oxygen pressure of 5×10^{-7} mbar (base pressure 3×10^{-10} mbar). Immediately after the film growth, both the NiO/MgO and the NiO/Ag samples were capped *in situ* with a protective 25 ML thick MgO overlayer. The thicknesses of both the NiO film and the MgO capping layer were calibrated by monitoring the intensity oscillations of reflection high energy electron diffraction

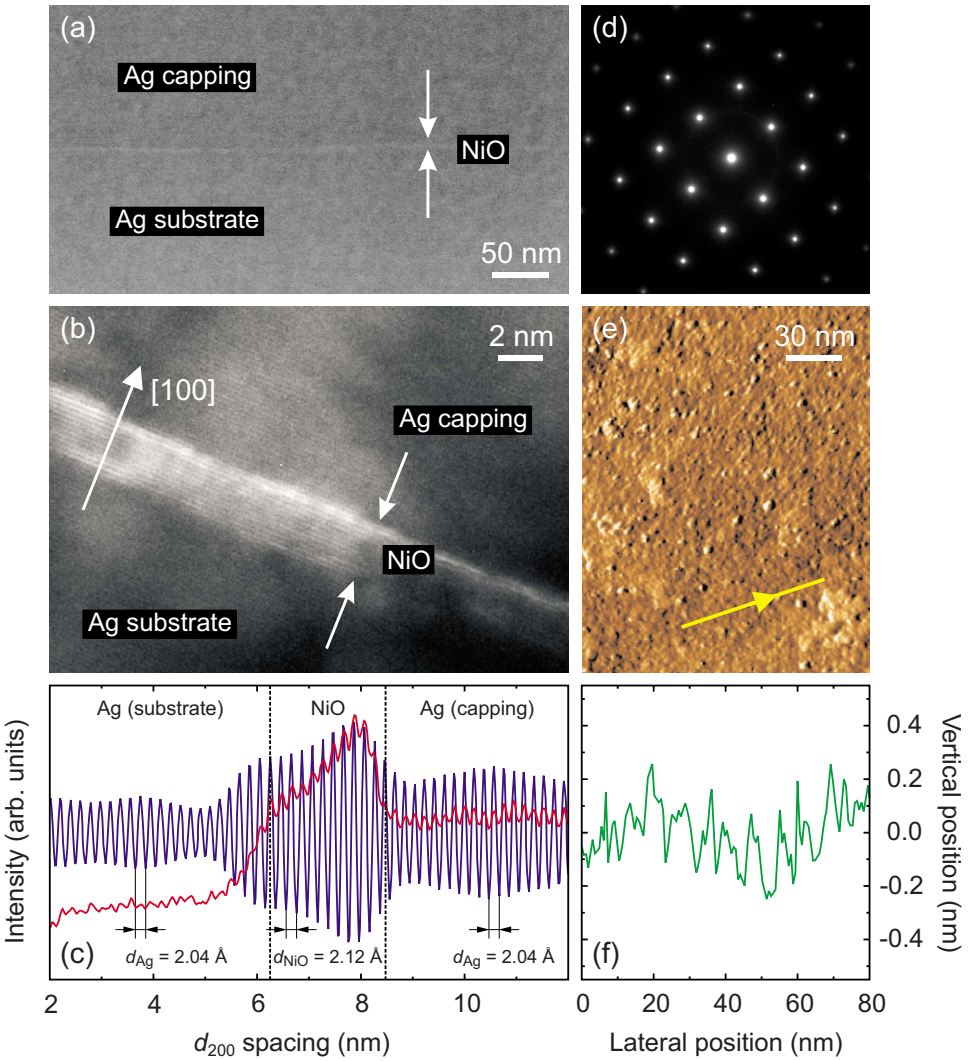

FIG. 1. (Color online) Ag/NiO/Ag cross sectional lamella: (a) SEM image; (b) HRTEM image; (c) HRTEM intensity line scan through Ag/NiO/Ag interfaces; (d) SAD pattern. (e) STM image of uncapped 3 ML NiO(100)/Ag(100) at $V=3$ V and $I=0.1$ nA. (f) STM intensity line scan along the line in panel (e).

(RHEED) in preceding NiO and MgO film growth experiments. *Ex situ* high-resolution transmission electron microscopy (HRTEM) measurements provided an independent absolute calibration of the NiO and MgO film thicknesses and a detailed structural characterization of 500 nm Ag(100)/2.3 nm NiO(100)/Ag(100) by studying cross sectional lamellae 80 nm thick obtained by focused ion-beam milling (FEI Strata 235DB) and lift-out extraction (Kleindeik MM3A micromanipulators), as shown in Fig. 1.

Figure 1(a) displays a cross sectional scanning electron microscopy (SEM) image of a Ag/NiO/Ag sandwich recorded at micrometric length scale showing that the NiO film covers uniformly the Ag(100) single crystal. Figure 1(b) displays a HRTEM image of the Ag/NiO/Ag sandwich where the atomic structure due to the (200) planes along the [100] direction is clearly resolved. Intensity line scans across the Ag/NiO/Ag interfaces are reported in Fig. 1(c). The thick (red online) and thin (blue online) lines were measured on the raw data and on the Bragg filtered image, respectively, and consistently give the same result: the fringes measured both in the Ag substrate and capping layer have identical spacing ($d_{Ag}=2.04$ Å) while those measured within the NiO film region have a larger average spacing ($d_{NiO}=2.12$ Å) by an amount $\varepsilon_{\perp}^{exp}=3.9\%$. The theoretically expected strain state of fully coherent NiO/Ag epitaxial film with tetragonal distortion is given by $\varepsilon_{\perp}^{th}=f\ (1+\nu)/(1-\nu)$, where $f=(a_{NiO}-a_{Ag})/a_{Ag}$ and ν is the NiO Poisson ratio.[38] Reported values of ν are between 0.21 (Ref. 31) and 0.30 (Ref. 32) which yield $\varepsilon_{\perp}^{th}$ between 3.4% and 4.1%, in good agreement with the measured value. The intensity profile in Fig. 1(c) also shows that the transition from Ag to NiO occurs over a length scale of about one lattice spacing. Figure 1(d) displays a selected area diffraction (SAD) pattern recorded with the HRTEM electron beam impinging over an area of about 1 μm centered on the NiO layer, showing the highly ordered crystal structure of the entire Ag/NiO/Ag sandwich. Figure 1(e) displays a scanning tunneling microscopy (STM) image of an uncapped 3 ML NiO/Ag film showing that the NiO layer covers uniformly flat silver terraces with an average surface roughness of 1.8 ± 0.2 Å. There are no signs in

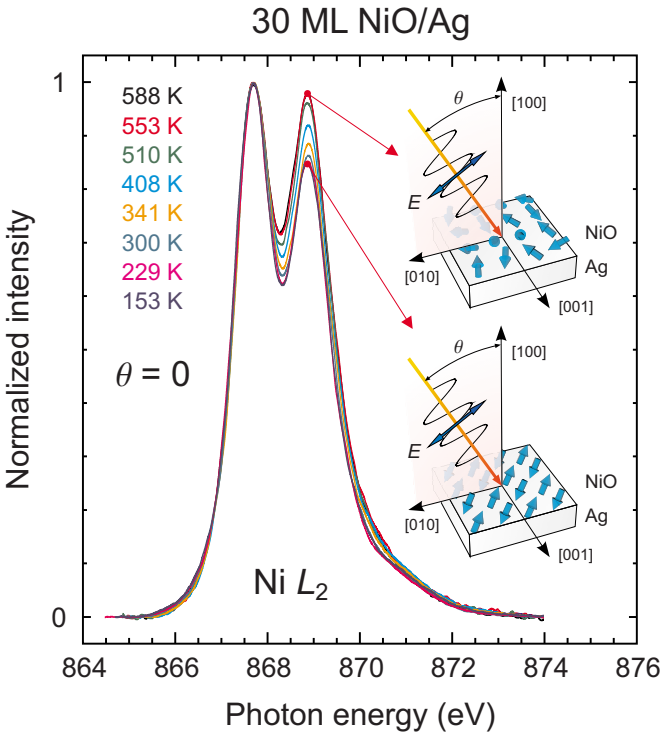

FIG. 2. (Color online) Temperature-dependent Ni L_2 XAS spectra with linearly polarized light at θ=0° on 20 ML MgO(100)/30 ML NiO(100)/Ag(100) and related changes in magnetic ordering.

Fig. 1(e) of three-dimensional NiO islanding on the Ag substrate, in agreement with the layered nature revealed by the SEM and HRTEM data in Figs. 1(a)–1(c).

In preparing the NiO/MgO system, we have followed the successful molecular-beam epitaxy (MBE)-reactive deposition method developed earlier.[8,29,31,37] We remark that the growth, structure, morphology, and properties of the NiO/MgO system have been extensively and thoroughly investigated both theoretically[35,36] and experimentally[8,29,31,33,34] by many groups through the years. In the literature, NiO/MgO was prepared by a variety of growth methods such as MBE-reactive deposition, rf-sputtering, and laser pulsed deposition, and its properties were analyzed by a wide variety of microscopy and electron spectroscopy techniques.[8,29,31,33,34] These studies coherently showed that nicely epitaxial NiO/MgO films can be prepared under a broad range of growth parameters such as substrate temperature (from 300 to 900 K) and oxidizing gas partial pressure (from ultrahigh-vacuum conditions to 10^{-6} mbar). In particular, there is a universal consensus in the literature about the NiO/MgO layer-by-layer growth mode, NiO/MgO surface and interface sharpness at atomic level, excellent epitaxy and atomic structure, and high thermal stability up to 600 K. Most of these good growth properties arise from the excellent lattice matching between NiO and MgO (lattice misfit $<1\%$). In particular, the HRTEM work by Kado[33,34] demonstrated the high epitaxial quality and sharpness of surface/interface in NiO(100)/MgO(100) films and Ag(100)/NiO(100)/MgO(100) superlattices. Indeed, the HRTEM data of Kado[33,34] constitute the NiO/MgO HRTEM counterpart of the HRTEM data reported in Fig. 1 for the NiO/Ag sample

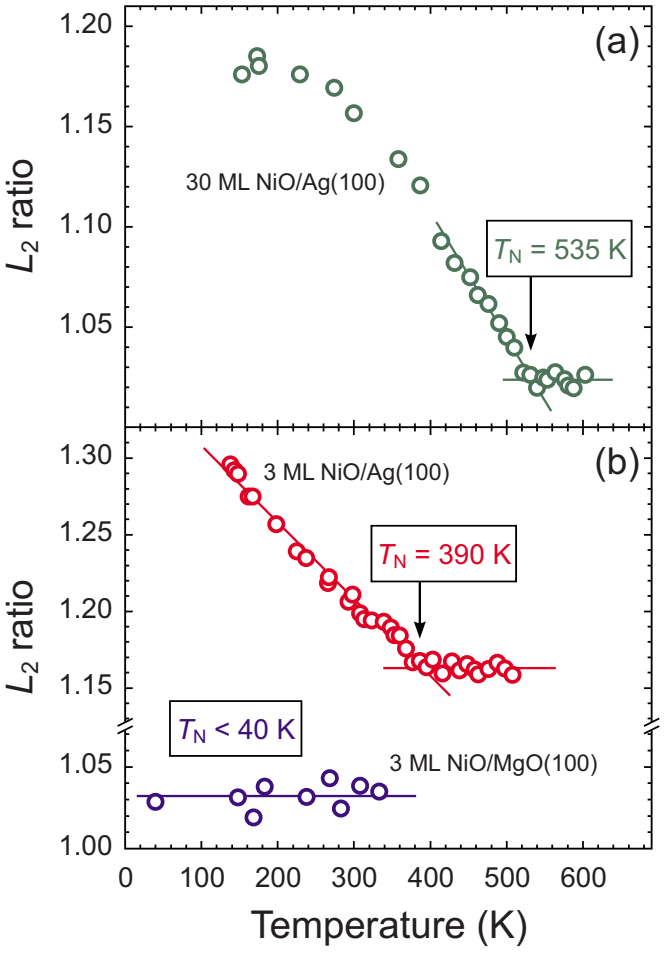

FIG. 3. (Color online) Temperature dependent Ni L_2 ratio of (a) 30 ML NiO(100)/Ag(100) and (b) 3 ML NiO(100)/Ag(100) (red markers) and 3 ML NiO(100)/MgO(100) (blue markers).

and show that the NiO/Ag and the NiO/MgO films are essentially identical as far as the NiO part is concerned, except for the different strain state.

III. RESULTS

To investigate the magnetic properties of these NiO thin films, we have utilized the magnetic linear dichroic (MLD) effect in the Ni L_2 x-ray absorption spectra (XAS). Experimental and theoretical studies in the last decade[8,39–45] have demonstrated that MLD-XAS is a very powerful method to investigate thin-film magnetic properties, especially as far as antiferromagnetic materials are concerned. To illustrate the application of this technique specifically for our case, we start with the XAS spectra for a 30 ML NiO/Ag film. Figure 2 displays the temperature dependence of the spectra recorded with linearly polarized light with the Poynting vector making an angle θ=0 with the sample surface normal and with the electric field **E** lying within the (001) plane. The intensity of the peak at 868.9 eV photon energy relative to that at 867.7 eV changes with temperature by about 15–20%. Although quite small, this effect is however highly reproducible and is at least 1 order of magnitude larger than the noise.

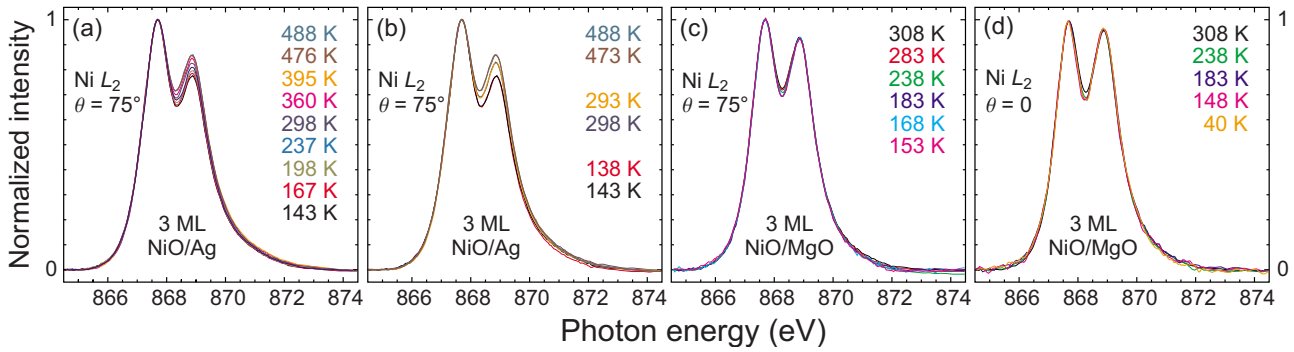

FIG. 4. (Color online) Temperature dependent Ni L_2 XAS spectra on [(a) and (b)] 25 ML MgO(100)/3 ML NiO(100)/Ag(100) and [(c) and (d)] 25 ML MgO(100)/3 ML NiO(100)/MgO(100) films.

The effect can thus be trusted and, following earlier work on NiO thin films on MgO,[8,40] can be associated with the occurrence of AF order. By plotting the intensity ratio between the two peaks at 867.7 and 868.9 eV (L_2 ratio) as a function of temperature, as done in Fig. 3(a), one obtains a direct measure of the long-range order parameter and the Néel temperature of the material. For the 30 ML NiO/Ag film we thus measure T_N=535 K, which is close to the bulk value of 523 K.[46] Apparently, the 30 ML NiO/Ag film is already thick enough to behave as the bulk oxide and not to feel any longer the influence of the underlying Ag substrate.[26,27]

Figure 4(a) displays the temperature dependent XAS spectra of the 3 ML NiO/Ag film with the Poynting vector making an angle θ=75° with the sample surface normal. The intensity of the peak at 868.9 eV relative to that at 867.7 eV clearly changes with temperature. It is important to stress that the spectra are highly reproducible also for this ultrathin NiO film. This is shown in Fig. 4(b) reporting the first spectrum measured at 298 K just after the film growth and the last spectrum measured at 293 K after six thermal cycles covering the range from 138 to 488 K. In the same panel we also show the spectra measured at T=473 K and T=143 K in the first thermal cycle and the corresponding spectra measured at T=488 K and T=138 K in the last thermal cycle proving the excellent thermal and chemical stabilities of the studied samples. The effect in Fig. 4(a) thus reflects the temperature dependence of the AF order. Fig. 3 reports the L_2 ratio as a function of temperature and it reveals that the Néel temperature of the 3 ML NiO/Ag film is T_N=390 K.

Figures 4(c) and 4(d) display the spectra of the 3 ML NiO/MgO film for temperatures between 40 and 308 K with θ=75° [Fig. 4(c)] and θ=0 [Fig. 4(d)]. Apart from a minor broadening effect with temperature, not much else is actually happening with the spectra. In particular, the intensity ratio between the two peaks at 867.7 and 868.9 eV is essentially temperature independent. In comparing the θ=75° to the θ=0 spectra, we also notice that the intensity ratio between the two peaks does not change, in very strong contrast with the case for 20 ML NiO/MgO.[8,40] All these suggest that there is no magnetic order in the 3 ML NiO/MgO, at least not in the measured temperature range. This, in turn, means that the Néel temperature T_N is dramatically suppressed, from 523 K for bulk NiO (Ref. 46) to well below 40 K for 3 ML NiO/MgO.

IV. DISCUSSION

The dramatic T_N reduction from the bulk NiO value T_N=523 K to T_N<40 K measured on 3 ML NiO/MgO is striking but not so unexpected. Indeed similar strong T_N reductions have been already reported for other 3*d* antiferromagnetic oxide ultrathin films and nanoparticles such as CuO,[2,4–6] CoO,[2,3] Co_3O_4,[7] and NiO (Refs. 3 and 8) supported on nonmagnetic insulating substrates. In particular, an earlier thickness-dependent study found T_N=470, 430, and 295 K for 20, 10, and 5 ML NiO/MgO films, respectively.[8] Several models have been proposed to describe these experimentally observed systematic reductions of magnetic ordering temperature starting from the basic idea of comparing film thickness (or particle size) to the spin-spin-correlation length. These models have been refined in a very recent paper[2] which generalizes previous theoretical approaches and establishes a simple and unified model that describes not only the thickness and size effect, but also the interface effects on the Néel temperature of antiferromagnetic thin films and nanocrystals supported on nonmagnetic insulating substrates. Based on these models, the Néel temperature of AF thin films and nanocrystals such as NiO, CuO, and CoO supported on nonmagnetic insulating substrates are predicted to strongly decrease with thickness and size. Indeed the calculated theoretical curve T_N versus film thickness/particle size fits nicely the experimentally measured T_N reductions of NiO, CuO, and CoO on nonmagnetic substrates (Figs. 6 and 7 in Ref. 2). Additional experimental confirmation of this drastic T_N suppression in AF oxide nanostructures due to finite-size effects is provided in Refs. 6 and 7 where reductions down to T_N=15 K are reported for AF CuO and Co_3O_4 nanoparticles with about 2 nm size. In particular, for NiO/MgO films the model fits nicely (Fig. 6 in Ref. 2) the experimentally observed[3,8] T_N reduction down to 300 K for 5 ML NiO/MgO and, even more important, all the proposed theoretical models reviewed in Ref. 2 coherently predict that a 3 ML NiO/MgO film should have a Néel temperature T_N <50 K (Fig. 6 in Ref. 2) as indeed observed in our work [Fig. 3(b)]. Therefore, the Néel temperature reduction down to T_N<40 K measured in our NiO/MgO sample can be reasonably interpreted as a genuine finite-size effect.

It is important to notice that, as discussed in Sec. II, our NiO/Ag and NiO/MgO films are essentially identical as far as the NiO part is concerned, except for the different type of

strain due to lattice mismatch which however, as thoroughly and quantitatively discussed below, does not significantly contribute to the different T_N value measured in NiO/MgO and NiO/Ag. As a consequence of this crucial point, and based on the observation that similarly to MgO also Ag is a nonmagnetic substrate, one would expect to measure exactly the same $T_N < 40$ K in both NiO/Ag and NiO/MgO, in striking contrast with our experimental observation that $T_N = 390$ K in NiO/Ag [Fig. 3(b)]. The origin of such a strongly different T_N value in NiO/MgO and NiO/Ag must thus be external to the 3 ML NiO film itself and must be searched in the different types of interactions at the NiO/MgO and NiO/Ag interfaces. These interactions must be such that the dramatic finite-size effects in these ultrathin films are manifest in NiO/MgO, but are efficiently counterbalanced in the NiO/Ag by another effect that can only be related to the presence of the Ag substrate. To discuss the origin of this extraordinary large T_N enhancement factor in the NiO/Ag compared to the NiO/MgO sample, we have to consider how the superexchange interactions in the NiO films are modified by the presence of the substrate. Using the well-known extended Anderson expression for the superexchange coupling constant J,[21–24]

$$J = -\frac{2t^4}{\Delta^2}\left(\frac{1}{\Delta} + \frac{1}{U}\right), \tag{1}$$

in which t is the anion $2p$–cation $3d$ transfer integral, Δ the $2p$-$3d$ charge-transfer energy, and U the on-site $3d$ Coulomb energy. One can expect that J, and consequently T_N, can be amplified by increasing t and/or decreasing Δ or U.

Already two decades ago, Duffy and Stoneham[28] predicted that a medium with a high dielectric polarizability should provide an effective screening for various charge excitations in a nearby located material. Indeed, Hesper *et al.*[25] and Altieri *et al.*[26,27,29] showed spectroscopically that the band-gap, the Hubbard-U, and the charge-transfer-Δ energies of an insulating material can be strongly reduced from its bulk values by depositing it as a thin film on top of a metal substrate. It has been estimated that this so-called image charge screening effect could result in a 50% reduction of U and Δ for NiO on Ag.[26] For NiO on MgO one can even envision an opposite effect: the polarizability of MgO is less than that of NiO, with the result that the U and Δ parameters in the NiO films are increased in comparison to the bulk values. Based on these large screening effects, it becomes almost obvious to expect a substantial enhancement of J and T_N in NiO/Ag compared to NiO/MgO, especially considering that U and Δ parameters enter as $1/(\Delta^2 U)$ and $1/\Delta^3$ into Eq. (1).

We notice that the use of hydrostatic pressure to reduce isotropically the interatomic spacing and thus to increase t is the conventional method to enhance superexchange interactions and the Néel temperature in many transition-metal oxides such as NiO, CoO, FeO, and MnO,[9–13] as well as to increase T_c's in various high-temperature superconductors.[13] Yet, the influences of modified t on J and T_N in our NiO/Ag and NiO/MgO films are negligible as we will show now using the theoretical[10] and experimental[11,12] lattice-dependent J and T_N values in NiO. For bulk NiO with $a_{NiO} = 4.10$ Å one obtains $J = 19.0$ meV and $T_N = 523$ K. If NiO is isotropically forced to fit the lattice constant of MgO or Ag, so that $a_{NiO} = a_{MgO} = 4.21$ Å or $a_{NiO} = a_{Ag} = 4.09$ Å, then $J^{MgO} = 18.42$ meV and $T_N^{MgO} = 507$ K or $J^{Ag} = 23.2$ meV and $T_N^{Ag} = 639$ K, respectively.[10–13] This would constitute an enhancement of both J and T_N by about a factor of 1.3 when comparing NiO/Ag to NiO/MgO, which is by far not enough to explain the contrast between the values $T_N = 390$ K and $T_N < 40$ K measured on NiO/Ag and NiO/MgO, respectively. Moreover, the strain in our films is nonisotropic and one could expect that the lattice spacing effect will be smaller since the change in the interatomic spacing along the surface normal is opposite to that in the film plane. Indeed, it has been experimentally shown that for NiO and CoO films on MgO uniaxial strain up to 2% has a negligible effect on T_N.[3]

Important for the modeling of our results are the findings of recent *ab initio* density-functional band-structure calculations on ultrathin NiO films, both free standing and supported on Ag(100).[47,48] The calculations predict that the magnetization and the superexchange constant J of 3 ML NiO films should hardly be affected by a nearby substrate. This shows that indeed T_N enhancement mechanisms based on an increase of t via the substrate should not play a major role. Moreover, this means that the explanation for the experimentally observed large discrepancy in T_N values for the NiO/Ag and NiO/MgO systems requires models which go beyond static mean-field theories. The screening model proposed here fulfills exactly this requirement: it explains the large differences in T_N and it is not captured by the standard band-structure calculations.

V. CONCLUSIONS

To conclude, using NiO/Ag and NiO/MgO as model systems, we have been able to show that screening by a metallic substrate provides a approach to restore magnetic ordering temperatures and superexchange interactions in ultrathin correlated oxide films well beyond the capability of conventional methods. We note, however, that image charge screening is not restricted to metals but is also present when using small-gap semiconductors with high dielectric polarizability. The proposed mechanism is presently ignored in available finite scaling theoretical calculations, it is not captured by the standard band-structure calculations, and requires models which go beyond static mean-field theories. Our results may point to a practical way toward designing strongly correlated oxide nanostructures with greatly improved magnetic ordering temperatures.

ACKNOWLEDGMENTS

We would like to thank G. A. Sawatzky for stimulating this work in several occasions. S.A. acknowledges CNR funding through project Short Term Mobility and financial support by CNR-INFM-S3 National Centre through project *Seed Activity*. The research in Köln is supported by the Deutsche Forschungsgemeinschaft through Grant No. SFB 608.

[1] M. Imada, A. Fujimori, and Y. Tokura, Rev. Mod. Phys. **70**, 1039 (1998).
[2] X. Y. Lang, W. T. Zheng, and Q. Jiang, Phys. Rev. B **73**, 224444 (2006).
[3] E. N. Abarra, K. Takano, F. Hellman, and A. E. Berkowitz, Phys. Rev. Lett. **77**, 3451 (1996).
[4] A. Punnoose, H. Magnone, M. S. Seehra, and J. Bonevich, Phys. Rev. B **64**, 174420 (2001).
[5] X. G. Zheng, T. Mori, K. Nishiyama, W. Higemoto, and C. N. Xu, Solid State Commun. **132**, 493 (2004).
[6] X. G. Zheng, C. N. Xu, K. Nishikubo, K. Nishiyama, W. Higemoto, W. J. Moon, E. Tanaka, and E. S. Otabe, Phys. Rev. B **72**, 014464 (2005).
[7] L. He, C. Chen, N. Wang, W. Zhou, and L. Guo, J. Appl. Phys. **102**, 103911 (2007).
[8] D. Alders, L. H. Tjeng, F. C. Voogt, T. Hibma, G. A. Sawatzky, C. T. Chen, J. Vogel, M. Sacchi, and S. Iacobucci, Phys. Rev. B **57**, 11623 (1998).
[9] D. Bloch, J. Phys. Chem. Solids **27**, 881 (1966).
[10] W.-B. Zhang, Y.-L. Hu, K.-L. Han, and B.-Y. Tang, Phys. Rev. B **74**, 054421 (2006).
[11] V. A. Sidorov, Appl. Phys. Lett. **72**, 2174 (1998).
[12] M. J. Massey, N. H. Chen, J. W. Allen, and R. Merlin, Phys. Rev. B **42**, 8776 (1990).
[13] T. Kaneko, H. Yoshida, S. Abe, H. Morita, K. Noto, and H. Fujimori, Jpn. J. Appl. Phys., Part 2 **26**, L1374 (1987).
[14] J.-P. Locquet, J. Perret, J. Fompeyrine, E. Mächler, J. W. Seo, and G. Van Tendeloo, Nature (London) **394**, 453 (1998).
[15] R. Bergholz and U. Gradmann, J. Magn. Magn. Mater. **45**, 389 (1984).
[16] Yi Li and K. Baberschke, Phys. Rev. Lett. **68**, 1208 (1992).
[17] F. Huang, M. T. Kief, G. J. Mankey, and R. F. Willis, Phys. Rev. B **49**, 3962 (1994).
[18] F. Wilhelm, U. Bovensiepen, A. Scherz, P. Poulopoulos, A. Ney, H. Wende, G. Ceballos, and K. Baberschke, J. Magn. Magn. Mater. **222**, 163 (2000).
[19] M. Przybylski and U. Gradmann, Phys. Rev. Lett. **59**, 1152 (1987).
[20] W. Weber, D. Kerkmann, D. Pescia, D. A. Wesner, and G. Guntherödt, Phys. Rev. Lett. **65**, 2058 (1990).
[21] P. W. Anderson, Science **235**, 1196 (1987).
[22] P. W. Anderson, Phys. Rev. **115**, 2 (1959).
[23] J. Zaanen, G. A. Sawatzky, and J. W. Allen, Phys. Rev. Lett. **55**, 418 (1985).
[24] J. Zaanen and G. A. Sawatzky, Can. J. Phys. **65**, 1262 (1987).
[25] R. Hesper, L. H. Tjeng, and G. A. Sawatzky, Europhys. Lett. **40**, 177 (1997).
[26] S. Altieri, L. H. Tjeng, F. C. Voogt, T. Hibma, and G. A. Sawatzky, Phys. Rev. B **59**, R2517 (1999).
[27] S. Altieri, L. H. Tjeng, F. C. Voogt, T. Hibma, O. Rogojanu, and G. A. Sawatzky, Phys. Rev. B **66**, 155432 (2002).
[28] D. M. Duffy and A. M. Stoneham, J. Phys. C **16**, 4087 (1983).
[29] S. Altieri, L. H. Tjeng, and G. A. Sawatzky, Thin Solid Films **400**, 9 (2001).
[30] S. D. Peacor and T. Hibma, Surf. Sci. **301**, 11 (1994).
[31] M. A. James and T. Hibma, Surf. Sci. **433-435**, 718 (1999).
[32] C. Giovanardi, A. di Bona, S. Altieri, P. Luches, M. Liberati, F. Rossi, and S. Valeri, Thin Solid Films **428**, 195 (2003).
[33] T. Kado, J. Appl. Phys. **78**, 3149 (1995).
[34] T. Kado, J. Cryst. Growth **144**, 329 (1994).
[35] M. D. Towler, N. M. Harrison, and M. I. McCarthy, Phys. Rev. B **52**, 5375 (1995).
[36] W. C. Mackrodt and C. Noguera, Faraday Discuss. **114**, 105 (1999).
[37] A. Rota, S. Altieri, and S. Valeri, Phys. Rev. B **79**, 161401(R) (2009).
[38] J. Hornstra and W. J. Bartels, J. Cryst. Growth **44**, 513 (1978).
[39] J. Stöhr, H. A. Padmore, S. Anders, T. Stammler, and M. R. Scheinfein, Surf. Rev. Lett. **5**, 1297 (1998).
[40] D. Alders, J. Vogel, C. Levelut, S. D. Peacor, T. Hibma, M. Sacchi, L. H. Tjeng, C. T. Chen, G. van der Laan, B. T. Thole, and G. A. Sawatzky, Europhys. Lett. **32**, 259 (1995).
[41] P. Kuiper, B. G. Searle, P. Rudolf, L. H. Tjeng, and C. T. Chen, Phys. Rev. Lett. **70**, 1549 (1993).
[42] H. Ohldag, T. J. Regan, J. Stöhr, A. Scholl, F. Nolting, J. Lüning, C. Stamm, S. Anders, and R. L. White, Phys. Rev. Lett. **87**, 247201 (2001).
[43] S. Altieri, M. Finazzi, H. H. Hsieh, H.-J. Lin, C. T. Chen, T. Hibma, S. Valeri, and G. A. Sawatzky, Phys. Rev. Lett. **91**, 137201 (2003).
[44] S. I. Csiszar, M. W. Haverkort, Z. Hu, A. Tanaka, H. H. Hsieh, H.-J. Lin, C. T. Chen, T. Hibma, and L. H. Tjeng, Phys. Rev. Lett. **95**, 187205 (2005).
[45] E. Arenholz, G. van der Laan, R. V. Chopdekar, and Y. Suzuki, Phys. Rev. Lett. **98**, 197201 (2007).
[46] G. A. Slack, J. Appl. Phys. **31**, 1571 (1960).
[47] S. Casassa, A. M. Ferrari, M. Busso, and C. Pisani, J. Phys. Chem. B **106**, 12978 (2002).
[48] F. Cinquini, L. Giordano, G. Pacchioni, A. M. Ferrari, C. Pisani, and C. Roetti, Phys. Rev. B **74**, 165403 (2006).